Experimental realization of a water-wave metamaterial shifter

C. P. Berraquero

Blackett Laboratory, Imperial College London, London SW7 2AZ, United Kingdom

A. Maurel

Institut Langevin LOA, UMR CNRS 7587-ESPCI, 5 rue Jussieu, 75005 Paris, France

P. Petitjeans

*Laboratoire de Physique et Mécanique des Milieux Hétérogènes (PMMH), UMR CNRS 7636-ESPCI-UPMC Univ.
Paris 6-UPD Univ. Paris 7, 10 rue Vauquelin, 75005 Paris, France*

V. Pagneux

Laboratoire d'Acoustique de l'Université du Maine, UMR CNRS 6613, Avenue Olivier Messiaen, 72085 Le Mans, France

We demonstrate by quantitative experimental measurements that metamaterials with anisotropic properties can be used in the context of water waves to produce a reflectionless bent waveguide. The anisotropic medium consists in a bathymetry with subwavelength layered structure that shifts the wave in the direction of the waveguide bending ($10°$, $20°$, and $30°$). The waveguide filled with such metamaterial is tested experimentally and compared to a reference empty bent waveguide. The experimental method used to characterize the wave field allows for space-time resolved measurements of water elevation. Results show the efficiency of the shifter. Modal treatment of the experimental data confirms that the metamaterial prevents higher modes from being excited in the waveguide.

The design of metamaterials has generated in the past 10 years a completely new, ever-changing field of study for electromagnetic, acoustic, elastic, and seismic waves [1–3]. Novel ways of applying wave field control have appeared such as the flat lens, the invisibility cloak, or the near zero index materials. The principle behind these metamaterials is to imagine a subwavelength structure specifically designed in order to procure certain material parameters for which the required wave propagation is obtained. The actual materials that have been built range widely depending of the original wave medium they are based on, as do the mathematical approaches. Amongst these different approaches, coordinate transformation theory (CTT) [4–6] allows us to find an anisotropic distribution of parameters that deviates waves without reflection. A medium with this particular anisotropic distribution of parameters can then be realized with homogenized microstructure by invoking effective medium theory (for the particular case of layered microstructure, see [7,8]). Structured media of propagation for water waves have been inspired mainly by photonic crystals, with emphasis on band gap properties [9–12]. Less attention has been generated by media with subwavelength microstructures leading to metamaterial behaviors [13–16]. This new type of wave control by metamaterials can be applied to, and is appealing in, every domain of wave physics. In particular, control of surface water waves might encourage applications in ocean and coastal engineering, which can include shore protection or energy harvesting.

In this paper, achievement of water-wave control using a transformation medium is demonstrated experimentally. The anisotropic medium is designed and developed to get a reflectionless bent waveguide which offers the capability to deviate the trajectory of water waves. We begin by considering the shallow-water-wave equation in a virtual (X,Y) space

$$\nabla \cdot (h_0 \nabla \eta) + \frac{\omega^2}{g}\eta = 0, \tag{1}$$

where $\eta(X,Y)$ is the vertical displacement of the water surface, ω is the angular frequency, g is the gravitational acceleration, and h_0 is the depth of water, assumed to be constant. We take here the shallow water limit $kh_0 \ll 1$, which implies that surface water waves will follow a dispersion relation $\omega = \sqrt{gh_0}k$.

According to the theory of transformation media, mapping of the coordinates $(X,Y) \to (x,y)$ (Fig. 1) results in a change of the parameters appearing in the wave equation (1). Denoting J the Jacobian tensor of the geometrical transformation, we obtain in the (x,y) real space [6]

$$\nabla \cdot [J h_0 \, {}^t J \, \nabla \eta] + \frac{\omega^2}{g}\eta = 0, \tag{2}$$

where we have considered a volume preserving transformation [$\det(J) = 1$]. Indeed, as already noted in [14], the wave equation can only support such transformations, given that the gravitational acceleration can not be tuned in usual situations. Amongst these kinds of transformations, the rotator system received particular consideration, including the publication of an experimental validation [8,14]. The transformation of the reflectionless wave shifter is also nonmagnetic (volume preserving) and corresponds to the change of coordinates $x = X$, $y = \tan\theta X + Y$ (Fig. 1), leading to the Jacobian

$$J = \begin{pmatrix} 1 & 0 \\ \tan\theta & 1 \end{pmatrix}. \tag{3}$$
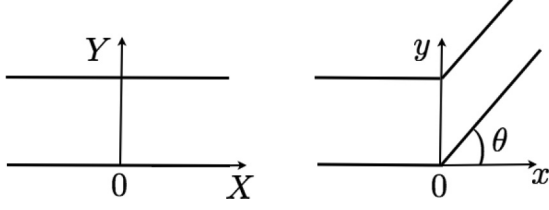
FIG. 1. Coordinate transformation of the shifter, from the virtual space (X,Y) to the real space (x,y).

Using the homogenization theory of layered medium, the anisotropy of the effective height $h_e \equiv J h_0 \, {}^t J$ can be reproduced using a layered structure composed by alternating layers of different heights, with some particular orientation in (x,y). In particular, with a structure consisting in layers of heights h_1 and h_2 and rotated by an angle α with respect to the x axis (Fig. 1), we obtain an anisotropic medium satisfying

$$\nabla \cdot \left[{}^t R_\alpha \begin{pmatrix} h_\parallel & 0 \\ 0 & h_\perp \end{pmatrix} R_\alpha \, \nabla \eta \right] + \frac{\omega^2}{g} \eta = 0, \qquad (4)$$

where $h_\parallel \equiv 2h_1 h_2/(h_1 + h_2)$ and $h_\perp \equiv (h_1 + h_2)/2$ and with R_α the conventional rotation matrix for a rotation by an angle α. Identifying Eqs. (2) and (4), we obtain $h_\parallel, h_\perp$ as the roots of $h^2 - (2 + \tan^2 \theta)h_0 h + h_0^2 = 0$ and $\sin 2\alpha = 2/\sqrt{4 + \tan^2 \theta}$. Thus, for a given angle θ of the shifter, the complete layered structure can be designed.

Now, we want to use the above transformation in a waveguide to produce a reflectionless bent guide. The boundary condition to be applied at the walls of the homogenized layered medium has been discussed in [17]. It is the same as the boundary condition in the transformed geometry (2) $(\mathbf{n} \cdot J \, {}^t J \nabla \eta = 0$, with $\mathbf{n}$ the normal to the wall). Remarkably, this condition is $\partial_y \eta = 0$ at the walls $y = \tan \theta x$ and $y = \tan \theta x + H$, which is counterintuitive with respect to the usual slip condition, but it allows the wavefronts to remains undistorted (along y) after the bend.

Three waveguides were built using rapid prototyping which were 70 mm in length, with a bend of angles $\theta = 10°$, $20°$, $30°$, respectively, as well as three reference empty waveguides of the same deviation angles [Fig. 2(b)]. For each of the three systems, we have (i) $\theta = 10°$: $h_1 = 1.842 \, h_0$, $h_2 = 0.543 \, h_0$, and $\alpha = 42.48°$; (ii) $\theta = 20°$: $h_1 = 2.467 \, h_0$, $h_2 = 0.405 \, h_0$, and $\alpha = 32.84°$; and $\theta = 30°$: $h_1 = 3.225 \, h_0$, $h_2 = 0.310 \, h_0$,
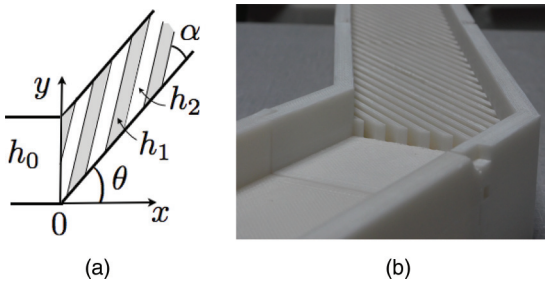

FIG. 2. (a) Bent waveguide: before the bend, the water height is h_0, and after the bend of angle θ, the metamaterial is realized with a layered structure with alternating layers of heights h_1 and h_2. (b) Designed metamaterial water waveguide.

and $\alpha = 36.95°$. As a compromise between the unwanted attenuation caused by small water depths and the wish to remain close to the shallow water approximation, we choose $h_0 = 10$ mm. In our working frequency range between 3 and 6 Hz, this leads to typical wavelengths between 40 and 90 mm. Obviously, the larger water depths h_1 resolve to values of $\tanh k h_1 / k h_1$ which go down to 0.2, largely out of the shallow water approximation which assumes $\tanh kh \to kh$. We will see that this does not have a significant impact on the efficiency of the metamaterial in our experiments. In our geometry, with such rapid variations of water height, a quantitative theory would have to include three dimensional, viscous, and weakly nonlinear effects. Finally, we design layers of 1 mm wide, sufficiently narrow with respect to the wavelength to expect the homogenization of the layered structure to be effective.

The waveguides are immersed in a water tank filled up to the initial water height $h_0 = 10$ mm. Waves of controlled frequency are obtained using an analog plane wave generator and they are sent at the entrance of the waveguides with zero incidence in order to generate only the mode 0 inside.

The experimental method used to quantify the wave field, Fourier transform profilometry (FTP) [18–23], is a technique based on fringe pattern projection on a surface and Fourier transform processing of the deformations of the fringe. A high resolution video projector (Epson TW5500) has been used to project over the measurement surface the fringe pattern whose deformation are recorded by a fast camera (Phantom v9.0). It allows us for time-resolved measurements of the water surface elevation at every point of the projected image, accurate to more than a millimeter. These measurements are used to build the complex wavefield at each working frequency. The real part of the wavefields before and after the bend of the waveguide are presented on Fig. 3 at $f = 4$ Hz. In the reference empty waveguides (without metamaterial), the effect of the bend is visible: even for a small deviation, the wavefield is composed of a combination of the mode 0 and of the mode 1, which is propagative at this frequency (the incident wavelength is about 76 mm). Inserting the metamaterial in the section of the waveguide after the bend has the expected effect: the scattering produced by the bend is almost suppressed in all cases. In transmission, the wave pattern matches our expectations: the wavefronts maintain their original direction (vertical in the representation of Fig. 3) and this is visible also near the walls. This means that the homogenization of the layered metamaterial is efficient even near the wall. Remark that, even if the shallow water approximation is questionable in the deeper layer of the metamaterial structure, the experimental results show that the whole structure behaves as expected by the homogenized shallow water theory. Finally, attenuation of the transmitted field is visible inside the metamaterial waveguide. This is due to the small water depth h_2 above the layered structure which produces the bottom friction responsible for the observed attenuation. With smaller and smaller depths h_2 needed for a higher bending angle, the attenuation increases with the angle θ.

To quantify the efficiency of the bent metamaterial guide, we carry out a modal analysis of the measured fields inside the waveguides, before and after the bend. The modal

(a) $\theta = 10°$
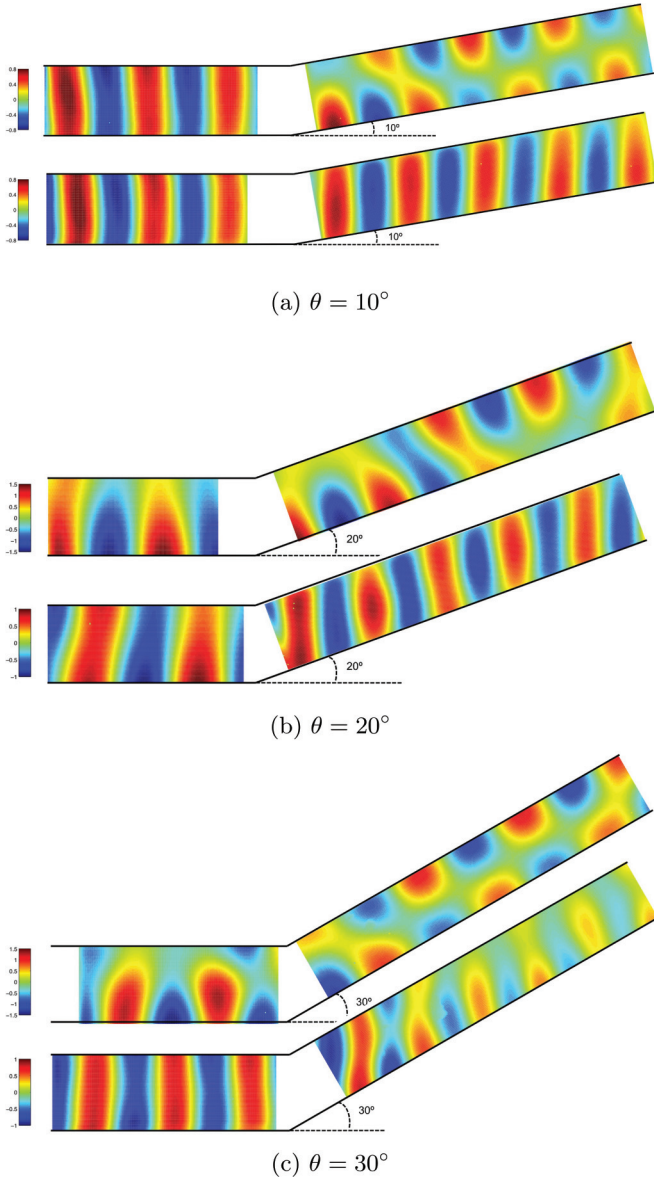

(b) $\theta = 20°$

(c) $\theta = 30°$

FIG. 3. (Color online) Real part of the measured fields of surface elevation in the reference empty waveguide without metamaterial (top) and in the metamaterial waveguide (bottom) at frequency $f = 4$ Hz. Then, waveguides have a bending angle of (a) 10°, (b) 20°, and (c) 30°.

decomposition is performed in the virtual space (X,Y):

$$\eta(X,Y) = \eta_0(X) + \sum_{n=1}^{\infty} \eta_n(X) \cos n\pi Y/H, \quad (5)$$

with

$$\eta_0(X) = \int_0^H dY \, \eta(X,Y),$$

$$\eta_n(X) = \sqrt{2} \int_0^H dY \, \eta(X,Y) \cos n\pi Y/H, \quad n > 0. \quad (6)$$

Before the bend, we simply have $(X = x, Y = y)$ and after the bend, the measured field $\eta(x,y)$ is interpolated on a grid (X,Y) built using the optical transformation $X = x$ and

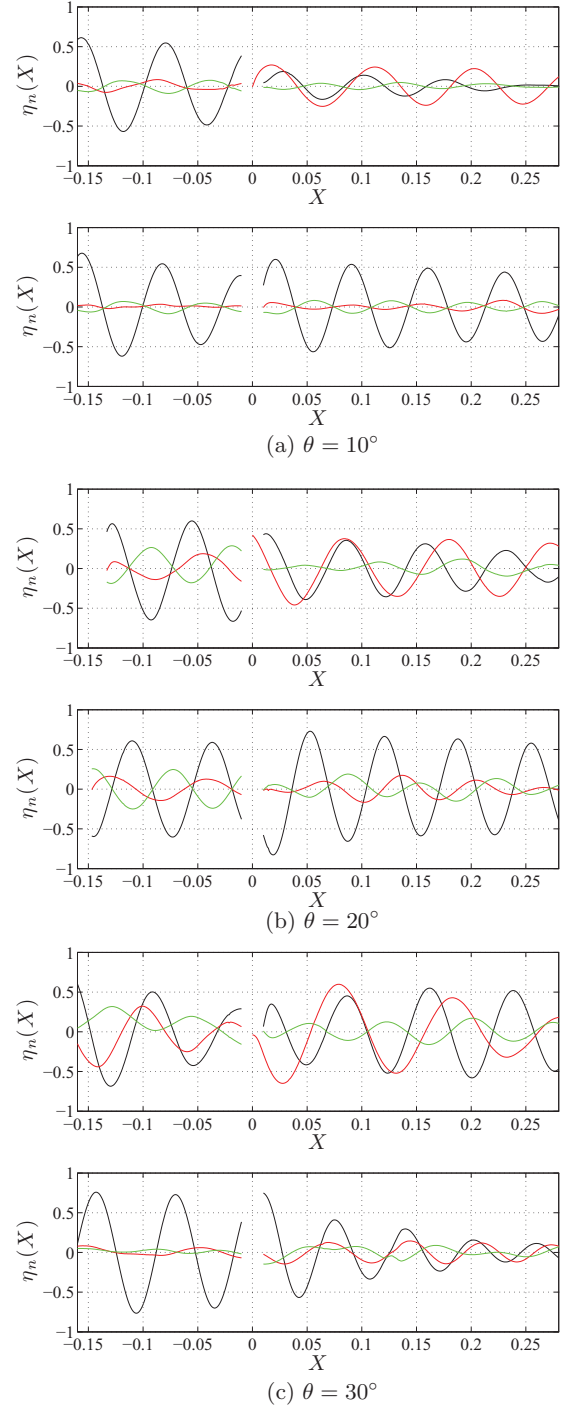(a) $\theta = 10°$

(b) $\theta = 20°$

(c) $\theta = 30°$

FIG. 4. (Color online) Modal components $\eta_n(X)$, $n = 0$ (black), $n = 1$ (red), and $n = 2$ (green) as a function of X (see text) before and after the bend. For each angle θ, the reference empty waveguide (top) and the waveguide with metamaterial (bottom) are shown.

$Y = y - \tan\theta x$. Figure 4 shows the results at $f = 4$ Hz (the first three propagative modes are shown).

Results confirm the qualitative observations drawn from Fig. 3. In the absence of a metamaterial, the bend produces the excitation of the higher modes $n = 1,2$. In the metamaterial waveguide, this effect is reduced and mode 0 remains largely dominant. The attenuation is visible in both cases but it is more acute in the metamaterial waveguide and the increase

of attenuation as θ increases is clear. For $\theta = 30°$, the amplitude of the waves has almost vanished at the waveguide outlet. Interestingly enough, we note that this makes the bent metamaterial waveguide a good candidate for an efficient "absorbing beach" since it behaves as a perfectly matched layer (i.e., without reflection). Indeed, it allows for the wave to leave the first part of the guide without backwards reflection and the attenuation ensures no reflection coming from the end of the bent part of the guide.

We measure the contribution of mode 0, $\eta_0(X)$, to the total field in reflection $X < 0$ and in transmission $X > 0$. To do that, we define

$$|\eta_0| \equiv \int dX \, |\eta_0(X)|, \quad |\eta| \equiv \int dX \int_0^H dY \, |\eta(X,Y)|.$$

The integrals are performed for $X < 0$ and we denote $r_R \equiv |\eta_0|/|\eta|$ the weight of mode 0 in reflection, and for $X > 0$ and we denote $r_T \equiv |\eta_0|/|\eta|$ the weight of mode 0 in transmission. These weight coefficients verify $0 \leqslant r_R \leqslant 1$ and $0 \leqslant r_T \leqslant 1$, where a weight equal to 1 corresponds to a wave with only mode 0. Results are shown in Fig. 5 as a function of frequency for the three angles $\theta = 10°, 20°, 30°$.

In all cases, the same tendencies are visible: in the low frequency limit, the mode 0 is always dominant. Moreover, a frequency increase in the reference empty waveguide results in the appearance of higher order modes which produce a decrease in the contribution of mode 0 to the total field. This appearance of higher order modes indicates that the scattering strength due to the bend increases. However, in the metamaterial waveguide, mode 0 remains largely dominant for all frequencies. This confirms the efficiency of the layered structure to produce a shifter effect in the bent guide. Besides, it is observed that the departure from shallow water approximation has no significant impact.

Our experiments show that it is possible to implement coordinate transformation metamaterials for surface waves in simple water. This contrasts with previous experiments where
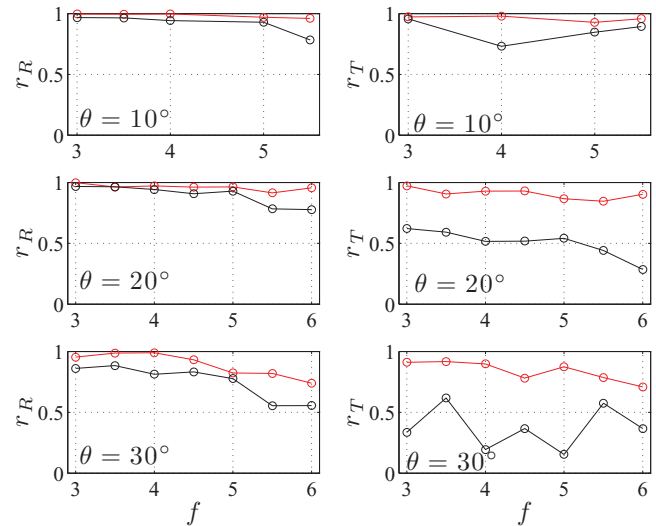

FIG. 5. (Color online) Contribution of mode 0 to the total field: left column, r_R in reflection ($X < 0$) and right column, r_T in transmission ($X > 0$) as a function of frequency. Red curves for the metamaterial waveguide and black curves for the reference empty waveguide.

the special liquids used are chosen for their low capillary effects or their low attenuations [13,14]. The efficiency of the layered structure to produce the shifter effect is quantitatively demonstrated owing to the space-time resolved measurements of the complete water wavefield. The shallow water approximation imposes nonmagnetic coordinate transformation where the water depth is the anisotropic parameter. Considering the full dispersion relation of water waves should allow for the possibility of using magnetic transformations.

[1] *Metamaterials: Physics and Engineering Explorations*, edited by N. Engheta and R. W. Ziolkowski (IEEE Press, Piscataway, NJ, 2006).

[2] *Metamaterials: Theory, Design, and Applications*, edited by T. J. Cui, D. R. Smith, and R. Liu (Springer, New York, 2009).

[3] R. V. Craster and S. Guenneau, *Acoustic Metamaterials Negative Refraction, Imaging, Lensing and Cloaking* (Springer, New York, 2013).

[4] J. B. Pendry, D. Schurig, and D. R. Smith, Science **312**, 1780 (2006).

[5] U. Leonhardt, Science **312**, 1777 (2006).

[6] U. Leonhardt and T. G. Philbin, Prog. Opt. **53**, 69 (2009).

[7] Y. Huang, Y. Keng, and T. Jiang, Opt. Express **15**, 11133 (2007).

[8] H. Chen and C. T. Chan, Phys. Rev. B **78**, 054204 (2008).

[9] X. Hu, Y. Shen, X. Liu, R. Fu, and J. Zi, Phys. Rev. E **69**, 030201 (2004).

[10] X. Hu and C. T. Chan, Phys. Rev. Lett. **95**, 154501 (2005).

[11] Y. Shen, K. Chen, Y. Chen, X. Liu, and J. Zi, Phys. Rev. E **71**, 036301 (2005).

[12] M. Farhat, S. Guenneau, S. Enoch, and A. Movchan, J. Comput. Appl. Math. **234**, 2011 (2010).

[13] M. Farhat, S. Enoch, S. Guenneau, and A. B. Movchan, Phys. Rev. Lett. **101**, 134501 (2008).

[14] H. Chen, J. Yang, J. Zi, and C. T. Chan, Europhys. Lett. **85**, 24004 (2009).

[15] X. Hu, C. T. Chan, K. M. Ho, and J. Zi, Phys. Rev. Lett. **106**, 174501 (2011).

[16] X. Hu, J. Yang, J. Zi, C. T. Chan, and K.-M. Ho, Sci. Rep. **3**, 1916 (2013).

[17] O. A. Oelinik, A. S. Shamaev, and G. A. Yosifian, *Mathematical Problems in Elasticity and Homogenization* (North Holland, Amsterdam, 1992).

[18] P. Cobelli, A. Maurel, V. Pagneux, and P. Petitjeans, Exp. Fluids **46**, 1037 (2009).

[19] A. Maurel, P. Cobelli, V. Pagneux, and P. Petitjeans, Appl. Opt. **48**, 380 (2009).

[20] A. Przadka, B. Cabane, V. Pagneux, A. Maurel, and P. Petitjeans, Exp. Fluids **52**, 519 (2011).

[21] G. Lagubeau, M. A. Fontelos, C. Josserand, A. Maurel, V. Pagneux, and P. Petitjeans, Phys. Rev. Lett. **105**, 184503 (2010).

[22] P. Cobelli, A. Przadka, P. Petitjeans, G. Lagubeau, V. Pagneux, and A. Maurel, Phys. Rev. Lett. **107**, 214503 (2011).

[23] A. Przadka, S. Feat, P. Petitjeans, V. Pagneux, A. Maurel, and M. Fink, Phys. Rev. Lett. **109**, 064501 (2012).